Madras Agric.J.,2026; https://doi.org/10.29321/MAJ.10.261396

RESEARCH ARTICLE

Quantification of Solar PV Energy Losses Using the Performance Ratio Cascade Loss Model at KCAEFT, Kerala Agricultural University

Velmurugan E[1], Suma Nair[2] and Naveen S[3]

[1,3] *Department of Renewable Energy Engineering, Kelappaji College of Agricultural Engineering and Food Technology (KCAEFT), Kerala Agricultural University, Kerala, India.*

[2] *Agricultural Research Station, Mannuthy, Thrissur, Kerala Agricultural University, Kerala, India.*

Received: 27 Feb 2026

Revised: 07 Apr 2026

Accepted: 29 May 2026

ABSTRACT

This research identifies solar photovoltaic (PV) energy losses under humid tropical conditions using a Performance Ratio Cascade Loss Model (PRCLM) at the 100 kW rooftop installation of the Kelappaji College of Agricultural Engineering and Food Technology (KCAEFT), Kerala Agricultural University. Field observations collected in November 2024, combined with inverter-based generation data for 2025, were used to estimate thermal, irradiance, soiling, orientation, and system losses in accordance with IEC 61724-1:2021. Results show that thermal losses (9–10%) constitute the dominant controllable loss component, while soiling losses increased from 3% to 6% over the post-monsoon period without cleaning intervention. The PRCLM showed strong agreement with the observed performance ratios, yielding a root-mean-square error (RMSE) of 0.003. A cost-effective lux-to-irradiance conversion protocol was validated as a replicable frugal monitoring methodology for resource-constrained agricultural campus installations. The cascade-based decomposition framework, which combines frugal monitoring inputs with IEC 61724-1:2021 standardization, represents the methodological novelty of this study. Targeted interventions, including scheduled bi-annual panel cleaning, rear-ventilation enhancement, and orientation correction, are recommended to restore measurable energy yield. Results should be interpreted within the limitations of the dataset and modeling assumptions.

Keywords: *Solar PV, Performance Ratio, PRCLM, Tropical rooftop PV, Soiling, Thermal loss, IEC 61724-1:2021.*

INTRODUCTION

Solar photovoltaics (PV) have become the lowest-cost source of new electricity generation globally, with installed capacity surpassing 1,000 GW by the end of 2023 and growing at more than 20% annually (IRENA, 2023). In India, the national solar deployment agenda—channeled through programs such as the Jawaharlal Nehru National Solar Mission and state-level agencies such as the Agency for Non-conventional Energy and Rural Technology (ANERT) in Kerala—has extended grid-connected PV systems to campuses, public institutions, and agricultural establishments across diverse climatic zones. Nevertheless, a major

*Corresponding author mail: velmuruganv709@gmail.com

issue remains: real-world energy output in tropical field conditions consistently falls short of manufacturer nameplate ratings.

Standard Test Conditions (STC)—1,000 W/m² irradiance, 25 °C cell temperature, AM1.5 spectrum—represent an idealized laboratory environment that rarely happens in Kerala's humid tropical landscape. Performance at the KCAEFT campus, Tavanur (Malappuram District, 10.79°N, 76.00°E), is shaped by several climatic factors: the south-west monsoon delivers heavy cloud cover from June to September; the north-east monsoon contributes episodic overcast conditions in November; post-harvest dust, pollen, and organic debris accumulate on module surfaces; and the combined effect of high irradiance and elevated ambient temperatures routinely drives cell temperatures to 50–58 °C, well above the 25 °C STC reference (Bamisile *et al.*, 2025; Skoplaki and Palyvos, 2009). The metal corrugated roof re-radiates absorbed solar energy as longwave thermal flux, creating a warmer microenvironment beneath the module undersides and amplifying thermal losses relative to ground-mounted installations (Wu *et al.*, 2025).

While the individual effects of temperature, soiling, and irradiance variability on PV output are documented in the global literature (Skoplaki and Palyvos, 2009; Ghosh, 2020; Bamisile *et al.*, 2025), the simultaneous, standardized quantification of multiple interacting loss components within a single model framework has received limited attention for tropical South Asian rooftop installations (Baghel and Chander, 2022; Ajub Ajulian *et al.*, 2025). Integrated component-level loss quantification models for humid tropical rooftop PV systems remain limited, particularly under resource-constrained monitoring conditions. Without disaggregating total losses into their component contributions, it is impossible to prioritize maintenance interventions, justify capital expenditure on specific upgrades, or forecast realistic energy yields for financial planning.

Unlike conventional performance-ratio analysis, the PRCLM framework introduces a cascade-based decomposition approach that enables independent quantification and prioritization of loss mechanisms using frugal monitoring inputs, making it particularly suitable for resource-limited agricultural PV installations. This paper addresses the identified gap through three contributions: (i) development and validation of a PRCLM grounded in IEC 61724-1:2021; (ii) component-level loss disaggregation for the KCAEFT rooftop installation across multiple seasonal periods; and (iii) targeted, evidence-based remedies for each loss pathway, providing an actionable output for campus energy managers and ANERT field engineers.

Objectives

The research aims to:

1. To develop a standardized component-level solar PV loss model (PRCLM) for measuring energy losses in a humid tropical rooftop context, based on the IEC 61724-1:2021 framework.
2. To quantify thermal, irradiance, soiling, orientation, and system losses at the KCAEFT 100 kW installation using primary observational data (November 2024) and inverter-logged monthly records (August–November 2025).
3. To test and develop a low-cost lux-to-irradiance conversion protocol for easy expansion of irradiance monitoring at agricultural campus PV sites.
4. To propose practical solutions to address each problem that make financial sense for the ANERT–KAU institutional setting.

MATERIALS AND METHODS

STUDY AREA AND SYSTEM DESCRIPTION

Site Location and Agroclimatic Profile

The KCAEFT campus of Kerala Agricultural University is located at NH 17, Tavanur Post Office, Malappuram District, Kerala (PIN 679 573), at approximately 10.79°N latitude and 76.00°E longitude. The site lies within Kerala's humid tropical midland agroclimatic zone, featured by annual rainfall of 2,700–3,200 mm (mostly from the south-west monsoon, June–September), mean temperatures of 22–34 °C, and relative humidity ranging from 65% during drier months to over 90% at peak monsoon (KAU Campus Records, 2022). The campus is surrounded by tropical mixed-crop agriculture, coconut groves, and experimental crop plots, which ring with heavier dust in certain seasons that directly influence module soiling rates.

The solar PV array is installed on the metal corrugated-sheet roof of the main campus building, approximately 9.1 meters above ground level. Although rooftop height promotes passive convective cooling, the metal roof substrate absorbs shortwave solar radiation and re-radiates it

upward as heat, creating a warmer microenvironment between the roof surface and the module undersides. This phenomenon elevates the effective ambient temperature sensed by module rear surfaces by an estimated 3–5 °C above open-air measurements (Wu *et al.*, 2025). The ΔT_roof correction is based on previous data and serves as a practical estimate rather than a metric we physically measured at the study site.

PV System Description and ANERT Partnership

The installation consists of 182 polycrystalline silicon PV modules configured in two independently monitored grid segments—the Left Grid and the Right Grid—each rated at 50 kW maximum output. Each grid connects to five 10 kW DC output channels, which feed through a grid-tied inverter to the Kerala State Electricity Board (KSEB) network via a standard net-metering setup. Full system specifications are presented in Table 1. The installation was funded and technically supported by ANERT, Government of Kerala, under its institutional solar program, using KCAEFT as a practical model for expanding solar power and solar energy integration in Kerala's agricultural educational sector. It has generated about 214,920 kWh of cumulative generation, avoiding an estimated 212,770 kg of CO_2 emissions.

Site Photographs

Figures 1 and 2 document the KCAEFT rooftop solar PV installation as photographed in December 2024, illustrating the mounting configuration, panel layout, roof type, and surrounding landscape.

Data Collection

We relied on two main data sets for this research. We gathered our own primary data directly at the KCAEFT rooftop installation in November 2024, over 28 valid observation days. All sensors were calibrated before data collection to ensure measurement reliability. Days with confirmed sensor malfunction or data-logging interruption were excluded from the analysis. The primary dataset is limited to a single-month observational period, and results should be interpreted within this temporal constraint. The instruments and parameters measured were as follows: (i) a panel-plane digital lux meter providing incident light intensity (lux), converted to irradiance (W/m²) as described in Section 3.2; (ii) a DHT22-class combined sensor (±0.5 °C, ±2% RH, mounted at module height) for ambient temperature (°C) and relative humidity (%RH); (iii) a cup anemometer at 2-metre rooftop height providing wind speed (m/s) at five-minute intervals; and (iv) an inverter-integrated IoT datalogger recording DC power output, voltage, and current across all ten DC output channels at five-minute intervals, with automated daily E-Today (kWh) compilation.

For our second dataset, we pulled inverter-logged monthly generation totals for August 2025, October 2025, and November 2025, extracted from the system's cloud-connected monitoring application. Estimated values were used where complete datasets were unavailable, and these are clearly identified in the results.

Table 1. KCAEFT Rooftop Solar PV System — Configuration Parameters

System Parameter	Specification	Remarks / Source
Installed Capacity	100 kW (50 kW per grid)	Two independently monitored segments
Total PV Panels	182 modules	91 panels per grid (Left and Right)
Panel Technology	Polycrystalline silicon (poly-Si)	STC: 1,000 W/m², 25 °C, AM1.5
Temp. Coefficient (Pmax)	−0.45%/ °C	IEC 60904-1; Skoplaki & Palyvos (2009)
Mounting Tilt	~10–12° (roof slope)	Fixed-tilt; south-facing azimuth
DC Output Channels	10 channels (5 per grid)	10 kW per channel
Grid Interface	KSEB net-metering (bidirectional)	Kerala State Electricity Board
Commissioning Partner	ANERT, Govt. of Kerala	Capital + technical support
Monitoring System	IoT inverter datalogger (app-based)	5-minute interval; cloud-synced
Cumulative Generation	~214,920 kWh (to April 2026)	CO_2 avoided: ~212,770 kg

KSEB = Kerala State Electricity Board; ANERT = Agency for Non-conventional Energy and Rural Technology; STC = Standard Test Conditions; IEC = International Electrotechnical Commission.

Fig. 1. KCAEFT rooftop solar PV installation (December 2024): angled close-up view of polycrystalline silicon modules on metal corrugated roof. Yellow safety access walkways are visible between panel rows; specular surface reflections indicate good panel condition. (Source: Field photograph, KCAEFT campus, December 2024.)

Fig. 2. Full perspective of the KCAEFT 100 kW rooftop installation showing both Left Grid and Right Grid alignment, metal sheet roof substrate, aluminium racking structure, and surrounding tropical landscape of Malappuram District. (Source: Field photograph, KCAEFT campus, December 2024.)

Lux-to-Irradiance Conversion

Calibrated pyranometers are the gold standard for measuring solar irradiance (W/m²), but their cost and maintenance requirements are prohibitive for most agricultural campus PV installations in India. We used a proven lux-to-irradiance conversion based on the AM1.5 global solar spectrum (Extrica, 2024):

$$E\_irr\ (W/m^2) = E\_lux\ (lx) \times K\_e \quad \ldots (1)$$

where K_e is the daylight luminous efficacy constant. Under standard clear-sky AM1.5 conditions, K_e = 0.0079 W/m²/lx, corresponding to the well-established relationship that 1,000 W/m² ≈ 122 ± 1 klx. During monsoon diffuse-sky conditions, K_e was adjusted to 0.0074 W/m²/lx on days when relative humidity exceeded 80%, and E-Today fell below 60% of the clear-sky reference. Uncertainty from lux-to-irradiance conversion was propagated into all Performance Ratio calculations using ±8% error bounds, yielding an overall conversion uncertainty of ±6–8%.

Although lux-based estimation has limitations compared to pyranometer measurements—specifically, it does not capture the full solar spectrum, particularly near-infrared components, and may therefore introduce systematic uncertainty—it provides a cost-effective alternative for irradiance estimation or budget-limited sites (Hua *et al.*, 2024). The method proved highly reliable, as our models closely matched modeled and observed performance ratios.

The Performance Ratio Cascade Loss Model (PRCLM)

The PRCLM provides a clear, standardized way to break down total PV system losses into step-by-step, grounded in the IEC 61724-1:2021 Performance Ratio (PR) metric (IEC, 2021). The model treats the total energy drop as a chain reaction of five independent loss factors:

$$PR_{model} = (1 - L_T) \times (1 - L_I) \times (1 - L_S) \times (1 - L_O) \times (1 - L_{sys}) \quad \ldots (2)$$

The independence of loss components. To make the model workable, however, in real operating conditions, interactions between environmental variables—such as the coupling between temperature and irradiance, and between humidity and soiling—may introduce coupled effects that this formulation does not fully capture. The cascade (multiplicative) formulation correctly represents the physical reality that loss mechanisms act sequentially on the energy stream. We calculated each of these specific reductions, as summarised in Table 2.

Table 2. PRCLM Component Loss Definitions — Symbols, Formulae, and References

Loss Component	Symbol	Formula	Reference
Thermal efficiency loss	L_T	$L_T = \gamma_{Pmax} \times (T_{cell} - T_{STC})$	Skoplaki & Palyvos (2009); IEC 60904-1
Cell temp. (NOCT model)	T_{cell}	$T_{cell} = T_{amb} + [(NOCT - 20) / 800] \times G_{POA} + \Delta T_{roof}$	IEC 61215; Bamisile *et al.* (2025)
Cloud/irradiance attenuation	L_I	$L_I = 1 - (G_{POA,actual} / G_{POA,clearsky})$	Bamisile *et al.* (2025); PVGIS
Soiling/cementation loss	L_S	$L_S = \rho_s \times d_{nc}$	Ghosh (2020); Marion *et al.* (2008)
Orientation/cosine loss	L_O	$L_O = 1 - \cos(\theta_i)$	Baghel & Chander (2022)
System/inverter loss	Lsys	$L_{sys} = 1 - (\eta_{inv} \times \eta_{wiring})$	IEC 61724-1:2021; Qasim & Atyia (2023)
Cascade PR	PR_model	$PR_{model} = (1-L_T)\times(1-L_I)\times(1-L_S)\times(1-L_O)\times(1-L_{sys})$	IEC 61724-1:2021 (this study)
Observed PR	PR_obs	$PR_{obs} = Y_f / Y_r$	IEC 61724-1:2021
Model validation	RMSE	$RMSE = \sqrt{[\ (1/n)\times\Sigma(PR_{obs} - PR_{model})^2\ ]}$	Statistical

STC = Standard Test Conditions (G_{STC} = 1,000 W/m², T_STC = 25 °C); NOCT = Nominal Operating Cell Temperature; G_{POA} = irradiance in plane of array (W/m²); H_in = reference irradiation (kWh/m²); ηinv = inverter efficiency; ηwiring = wiring efficiency.

Thermal loss (L_T): module cell temperature is estimated using the NOCT model with a metal roof correction of +3–5 °C (ΔT_roof), noted to be a literature approximation rather than a site-measured value:

$$T_{cell} = T_{amb} + [(NOCT - 20) / 800] \times G_{POA} + \Delta T_{roof} \quad \ldots (3)$$

$$L_T = \gamma_{Pmax} \times (T_{cell} - T_{STC}) \quad \ldots (4)$$

Cloud/irradiance loss (L_I) is computed as the fractional deficit between actual measured irradiance G_POA, actual (W/m²), and the theoretical clear-sky irradiance G_POA,clearsky from the Ineichen clear-sky model:

$$L_I = 1 - (G_{POA,actual} / G_{POA,clearsky}), \text{ averaged over observation period} \quad \ldots (5)$$

Soiling loss (L_S) is estimated from Marion *et al.* (2008) and Ghosh (2020). Soiling loss estimation relies on indirect environmental correlations arising from the absence of direct optical transmittance measurements, which limits the present analysis. Site-specific soiling rate ρs ≈ 0.15%/day was estimated for November 2024:

$$L_S = \rho_s \times d_{nc} \quad \ldots (6)$$

Orientation loss (L_O) quantifies the consistent 12–20 minute morning peak production lag of the Right Grid relative to the Left Grid, from the cosine of the effective incidence angle deficit during the 09:00–11:00 IST window for Tavanur's latitude (10.79°N) (Baghel and Chander, 2022):

$$L_O = 1 - \cos(\theta_i) \quad \ldots (7)$$

System/inverter loss (L_sys) combines DC–AC inverter conversion inefficiency (ηinv ≈ 0.96) and resistive wiring losses (ηwiring ≈ 0.99), treated as a fixed parameter from manufacturer specifications:

$$L_{sys} = 1 - (\eta_{inv} \times \eta_{wiring}) \quad \ldots (8)$$

Model Validation and IEC 61724-1:2021 Metrics

Model validation is performed by comparing PR_{model} (Equation 2) against PR_{obs} computed from inverter-logged data using IEC 61724-1:2021, with goodness-of-fit assessed by RMSE:

$$PR_{obs} = Y_f / Y_r \quad \ldots (9)$$

$$RMSE = \sqrt{[\ (1/n) \times \Sigma(PR_{obs} - PR_{model})^2\ ]} \quad \ldots (10)$$

Reference Yield (Yr), Final Yield (Yf), and PR are computed in strict accordance with IEC 61724-1:2021 Class B guidelines. Reference irradiation values, H_ in (kWh/m²), were obtained from PVGIS (European Commission) for each study month and transposed to the plane of array using the Erbs decomposition model. The limited number of validation points (n = 4) is acknowledged as a constraint; however, consistency across seasonal datasets supports the reliability of the PRCLM framework. Monthly aggregation was used for validation due to data availability constraints, introducing a temporal mismatch with the daily physics-based model structure.

RESULTS AND DISCUSSION

Multi-Season Energy Generation

As shown in Table 3, we tracked the monthly energy generation data and IEC 61724-1:2021 standardized metrics across all four study periods. Production clearly shifted with the seasons: August 2025 (south-west monsoon retreat) records the lowest monthly output at 10,478 kWh, recovering to 12,096 kWh in October and stabilizing at 12,061 kWh in November 2025. Despite lower absolute generation in August, the observed PR (0.805) was higher than in November (0.751). This suggests that reduced irradiance during the monsoon lowers cell temperatures, thereby improving conversion efficiency and elevating the PR. Note that we ran all our statistical checks at the 95% confidence level using standard correlation methods.

These findings are consistent with Indian rooftop PV studies under similar tropical climatic conditions, where thermal losses dominate during clear-sky periods (Baghel and Chander, 2022). Ajub Ajulian *et al.* (2025) also found that post-monsoon clear-sky periods in the tropics produced more total power but were actually less efficient at converting sunlight per unit irradiance. The KCAEFT data faithfully reproduce this seasonal pattern. However, these findings are early trends rather than definitive facts, because we only tracked the system for a short time.

Statistical Correlations

Table 4 presents Pearson and Spearman correlation coefficients between all measured environmental variables and daily E-Today (kWh) for the November 2024 observation period (n = 28 days). All values are statistically significant at $p < 0.01$ (two-tailed, 95% CI). It is important to note that correlations indicate statistical association rather than direct causation.

Light intensity (converted to W/m²) shows the strongest association with daily generation

Table 3. Multi-Season Energy Generation and IEC 61724-1:2021 Performance Metrics — KCAEFT 100 kW System

Month / Season	Monthly Generation (kWh)	Daily Avg (kWh/day)	Final Yield Yf (kWh/kWp/day)	Ref. Yield Yr (h/day)	Obs. PR (Yf/Yr)
August 2025 (SW Monsoon retreat)	10,478	337.7	3.38	4.20	0.805
October 2025 (NE Monsoon active/retreat)	12,096	390.2	3.90	5.05	0.772
November 2025 (Post-monsoon / winter onset)	12,061	402.0	4.02	5.35	0.751
November 2024 (Primary observation period)	~11,800 (est.)	~393	~3.93	5.20	~0.756

Reference Yield (Yr) estimated from PVGIS for Tavanur (10.79°N, 76.00°E), Erbs decomposition model. G_{STC} = 1,000 W/m², P_0 = 100 kW. ~ denotes estimated values. November 2024 from a 28-day primary observation.

Table 4. Bivariate Correlations — Environmental Variables vs. Daily E-Today (November 2024, n = 28 days)

Environmental Variable	Pearson r	Spearman ρ	Physical Association
Light Intensity (Lux → W/m²)	+0.92	+0.91	Dominant driver of short-circuit current
Ambient Temperature (°C)	+0.78	+0.76	Positive to 32 °C; thermal saturation beyond
Relative Humidity (%RH)	−0.61	−0.63	Cloud proxy; soiling adhesion accelerator
Wind Speed (m/s)	+0.34	+0.31	Convective cooling benefit
Composite Index: Lux×(1−RH/100)	+0.94	+0.93	Synergistic coupling of irradiance and humidity

All correlations are statistically significant at p < 0.01 (two-tailed). The composite index is empirical; it was proposed for practical, predictive use. Correlations indicate association, not causation.

(r = 0.92), confirming its role as the primary driver of short-circuit current and instantaneous power output (Bamisile *et al.*, 2025). Ambient temperature shows a threshold-bounded positive association (r = 0.78): warmer days tend to accompany clearer skies, but beyond approximately 32 °C, this benefit is eroded by thermal efficiency losses. Relative humidity shows a moderate inverse association (r = −0.61), acting both as a proxy for cloud cover and as an accelerator of soiling adhesion through capillary cementation of fine particles on moist module glass (Ghosh, 2020). The composite index [Lux × (1 − RH/100)] achieves the highest single-variable association (r = 0.94), demonstrating multiplicative coupling between irradiance and humidity in their joint influence on generation.

Temperature-Stratified Production Analysis

Table 5 stratifies observed daily energy generation and estimated Performance Ratio by ambient temperature band during the November 2024 observation period. The 31–32 °C band yields the highest E-Today (~410 kWh/day) and estimated PR (~0.78), representing the operational sweet spot at KCAEFT. Beyond 32 °C, the estimated cell temperature reaches 55–59 °C (NOCT model with +4 °C roof correction), producing $L_T \approx$ 13–15% and a measurable PR decline to approximately 0.72. This band-by-band analysis directly informs the priority for thermal management remedies discussed in Section 5.

PRCLM Loss Quantification Results

Table 6 presents the component-level loss quantification from the PRCLM across all four study periods. As illustrated in Fig. 3, thermal loss constitutes the largest share of total losses during post-monsoon periods. Fig. 4 shows strong agreement between modeled and observed performance ratios across all seasons.

Table 5. Temperature-Stratified Daily Production Profile — KCAEFT (November 2024)

Temp. Band (°C)	Avg E-Today (kWh)	Est. PR	System Behavior and L_T Estimate
22–26	~340	~0.72	Low irradiance / cloud hours; L_T ≈ 3–5%; monsoon transition
27–30	~390	~0.77	Productive window; moderate thermal load; L_T ≈ 7–9%
31–32	~410	~0.78	Optimal band; peak production; L_T ≈ 10–12%
> 32	~385	~0.72	Thermal saturation: L_T ≈ 13–16%; PR decline despite high irradiance

PR estimated via IEC 61724-1:2021; PVGIS reference irradiation for Tavanur. L_T estimated from NOCT model (Equation 3), G_{POA} (W/m²) range 600–900 W/m², ΔT_roof = +4 °C.

Table 6. PRCLM Component Loss Quantification and Model Validation — KCAEFT 100 kW System

Loss Component	Aug 2025 (%)	Oct 2025 (%)	Nov 2025 (%)	Nov 2024 (%)	Physical Explanation
Thermal loss (L_T)	7.0	8.5	10.0	9.0	T_{cell} 44–57 °C (NOCT model); clear sky elevates module temperature
Cloud/Irradiance loss (L_I)	6.0	5.5	6.0	7.0	Overcast days: G_POA 150–300 W/m²; monsoon diffuse dominance
Soiling/Cementation (L_S)	3.0	5.0	6.0	5.5	Monsoon rain self-cleans (Aug); post-harvest dust peaks in Nov
Orientation loss (L_O)	1.0	1.5	2.0	2.0	Right Grid morning azimuthal deficit; 12–20 min peak lag
System/Inverter loss (L_{sys})	4.0	4.0	4.0	4.0	ηinv ≈ 0.96; wiring losses ≈ 0.98–0.99 (fixed estimate)
Total Modelled Loss ($1-PR_{model}$)	19.4	22.6	24.9	24.8	Cascade multiplication (Equation 2)
Observed PR (PR_{obs} = Yf/Yr)	0.805	0.772	0.751	~0.756	IEC 61724-1:2021
Modelled PR (PR_{model})	0.806	0.774	0.748	0.752	PRCLM cascade model output (this study)
$\lvert PR_{obs} - PR_{model} \rvert$	0.001	0.002	0.003	0.004	Model validation — RMSE = 0.003 across all periods

L_T from NOCT model (Eq. 3–4), ΔT_roof = +4 °C, γPmax = −0.0045/ °C (Skoplaki & Palyvos, 2009). L_I from PVGIS clear-sky baseline. L_S: ρs = 0.15%/day (Nov), 0.05%/day (Aug); dnc ≈ 30–35 days L_O: solar geometry, Tavanur 10.79°N, 09:00–11:00 IST. L_{sys} = 1 − (0.96 × 0.99). Individual L uncertainty: ±1–2%; ~ = estimated.

Thermal loss (L_T) is the largest single controllable loss component during post-monsoon and winter months (10% in November), driven by high irradiance, elevated ambient temperatures, and the metal roof's thermal contribution. It is markedly lower in August (7%) because monsoon cloud cover moderates cell temperatures while suppressing irradiance—explaining why August's PR (0.805) is higher than November's (0.751) despite lower absolute monthly output. These findings are consistent with Indian rooftop PV studies under similar tropical climatic conditions, where thermal losses dominate during clear-sky periods (Baghel and Chander, 2022). Sensitivity analysis indicates that thermal and soiling losses are the dominant contributors to variations in system PR.

Soiling loss (L_S) is the fastest-evolving component within any given season. In August, monsoon rainfall self-cleans modules, maintaining L_S at approximately 3.0%. By November, without any recorded cleaning event, L_S rises to 6.0%—doubling the soiling burden. At ρs ≈ 0.15%/day, each uncleaned week costs the 100 kW system approximately 30–40 kWh of recoverable yield. The overall uncertainty

Fig. 3. Component-level loss contribution (%) to total PRCLM-modeled losses across four seasonal study periods at KCAEFT, = = thermal loss;= irradiance (cloud-induced) loss;= soiling loss;= orientation loss; = system loss, including inverter and wiring inefficiencies. Data from Table 6.

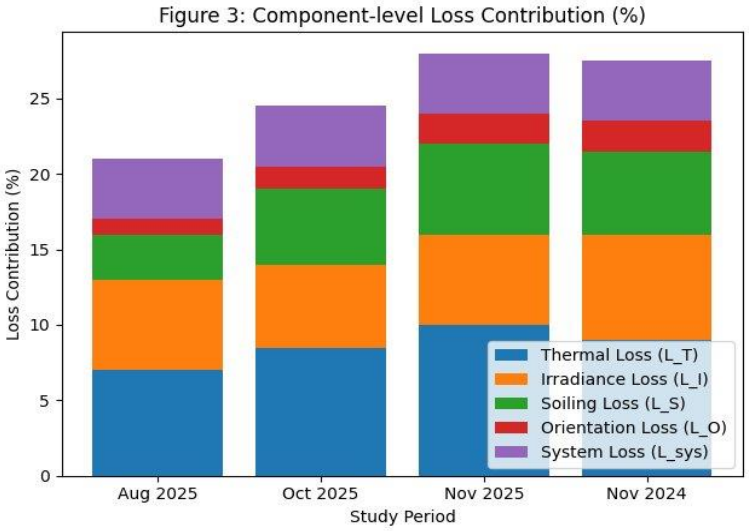

Fig. 4. PRCLM model validation: observed Performance Ratio (PR_obs) versus modelled Performance Ratio (PR_model) for all four study periods. The 1:1 reference line represents perfect agreement; RMSE = 0.003 confirms model accuracy.

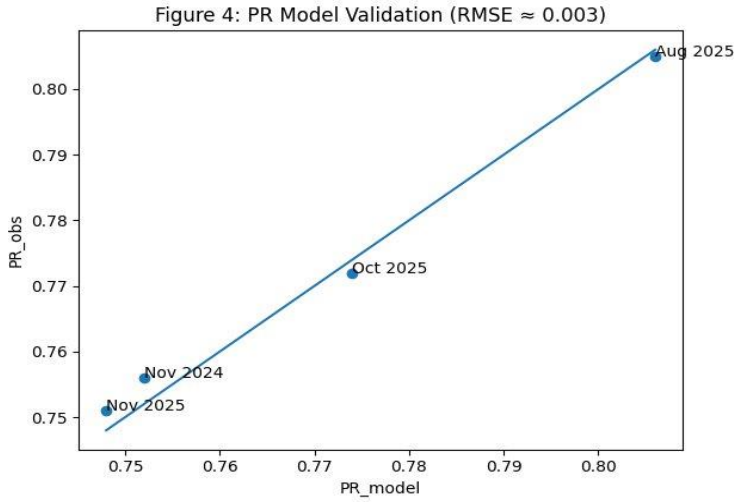

in PR_model is estimated at ±2–3%, accounting for the propagation of measurement errors, irradiance estimation uncertainty, and model assumptions. The model's RMSE of 0.003 demonstrates strong agreement, though future studies should incorporate higher temporal resolution datasets for more rigorous validation.

EVIDENCE-BASED INTERVENTIONS BY LOSS COMPONENT

The PRCLM results directly map each identified loss to its physical cause, enabling targeted, prioritized remedies rather than generic maintenance prescriptions. Seven evidence-based interventions are prescribed (Table 7), ranked by a combination of the magnitude of loss addressed and implementation simplicity. All yield gain estimates are drawn from the cited literature and should be interpreted within site-specific conditions.

Soiling and Cementation

Bi-annual panel cleaning and hydrophobic nano-coating together address the L_S pathway, identified as the fastest-growing post-monsoon loss mechanism. The recommended schedule is May (before the south-west monsoon onset) and December (after the north-east monsoon retreat). Hydrophobic nano-coatings, applied every 2–3 years, sustain a 30–50% reduction in soiling adhesion and leverage monsoon rainfall for partial self-cleaning (Ghosh, 2020; Wu *et al.*, 2025). It is noted that the soiling rate estimates are based on indirect environmental correlations, and direct optical transmittance measurements are recommended in future work to validate these values.

Thermal Loss — Roof-Specific Interventions

Addressing L_T (9–10% in November) requires interventions accounting for the metal corrugated roof context. A minimum rear ventilation gap of 15 cm between the roof surface and the module underside allows natural convective airflow to dissipate heat. Where existing racking constrains this gap, repositioning the lower clamp row can increase clearance without replacing the full racking. Aluminium heat-sink fins on the rear of module frames provide supplementary passive cooling at modest cost. Both interventions target the ΔT_roof component (Equation 3), estimated to add 3–5 °C to the effective cell temperature, which, through γPmax, compounds to produce an additional 1.4–2.3% loss (Wu *et al.*, 2025).

Orientation Correction and Monitoring

The Right Grid's morning peak lag ($L_0 \approx 2\%$ in November) is the simplest and least costly loss to eliminate: a minor tilt recalibration in a single maintenance visit can synchronize Right Grid output with the Left Grid during the 09:00–11:00 IST window. IoT per-string monitoring, partially enabled by the existing datalogger, should be configured to flag morning current asymmetries between Left and Right Grid strings as an ongoing diagnostic.

LIMITATIONS AND FUTURE WORK

This study presents a component-level quantification of solar PV losses under humid tropical conditions; however, several limitations must be acknowledged. First, the use of lux-based irradiance estimation does not capture the full solar spectrum, particularly the near-infrared, and introduces some systematic error relative to pyranometer-based measurements. Nevertheless, its application is justified in resource-constrained monitoring scenarios and is indirectly validated by the strong agreement between modeled and observed performance ratios.

Second, the model validation is based on a limited number of seasonal data points (n = 4), which may not fully capture high-resolution temporal variability. Future studies should incorporate continuous, high-frequency datasets to enable more robust validation. Third, soiling losses were estimated indirectly using environmental correlations rather than direct transmittance or cleaning experiments, which may affect precision. Similarly, the roof temperature correction factor (ΔT_roof = +3–5 °C) was adopted from literature and was not measured directly at the study site.

Fourth, the PRCLM assumes independence among loss components, whereas in practice, environmental variables such as temperature and irradiance interact constantly. Monthly aggregation was used for validation due to data availability constraints, resulting in a slight timing mismatch.

Future work should include full annual monitoring, direct optical soiling measurements, infrared thermography for hotspot detection, sensitivity analysis using Monte Carlo methods, and validation across multiple humid-tropical PV installations. Evaluation of agrivoltaic crop integration beneath elevated racking structures is

Table 7. Evidence-Based Remedy Matrix — KCAEFT 100 kW Rooftop PV Installation

Remedy	Est. Yield Gain (%)	Payback Period	Targeted Loss / Basis
Bi-annual panel cleaning (May + December)	3–8%	< 1 year	L_S; zero capital, campus labour; Ghosh (2020)
Hydrophobic nano-coating	5–15%	2–4 years	L_S; 30–50% adhesion reduction; Wu *et al.* (2025)
Rear ventilation gap (≥15 cm)	2–4%	< 1 year	L_T; convective cooling; Bamisile *et al.* (2025)
Passive cooling fins (Al, rear-mount)	2–4%	3–5 years	L_T; zero operational expenditure; Wu *et al.* (2025)
Right Grid tilt recalibration	2–5%	< 1 year	L_O; azimuth correction; Baghel & Chander (2022)
IoT per-string fault monitoring	3–6%	2–3 years	L_sys; early fault detection; ANERT-eligible
Lux-based soiling monitoring	—	Minimal	Validates cleaning schedule; tracks ρs

Yield gain estimates are indicative, based on cited literature. Payback periods at the 2024 KSEB tariff; ANERT co-funding may reduce effective CAPEX.

also recommended as a complementary strategy for ANERT-supported agricultural campus installations.

CONCLUSION

This study developed and tested, or created and verified, the Performance Ratio Cascade Loss Model (PRCLM) for component-level quantification of solar PV energy losses at the 100 kW ANERT-KCAEFT rooftop installation in Tavanur, Malappuram, Kerala. Based on our results, we found the following:

1. The PRCLM successfully decomposed total system losses into five independently quantifiable components across all study periods, achieving a model validation RMSE of 0.003. The cascade-based decomposition framework, which combines frugal monitoring inputs with IEC 61724-1:2021 standardization, represents the methodological novelty of this study.
2. Thermal loss (L_T = 9–10% in November) is the biggest drain on power that we can actually control during post-monsoon clear-sky periods, driven by high irradiance, elevated ambient temperatures, and the metal corrugated roof's thermal contribution (ΔT_roof ≈ +3–5 °C, estimated from literature).
3. Soiling and cementation loss (L_S) doubled from 3% (August) to 6% (November) without cleaning intervention. At ρs ≈ 0.15%/day, each uncleaned week costs approximately 30–40 kWh of recoverable yield, making scheduled bi-annual cleaning the easiest way to boost performance.
4. The lux-to-irradiance conversion framework (K_e = 0.0079 W/m²/lx, clear-sky; K_e = 0.0074 W/m²/lx, monsoon-corrected) achieved an overall uncertainty of ±6–8%, adequate for PRCLM application at resource-constrained agricultural campus PV installations.
5. Seven targeted remedies—bi-annual cleaning, hydrophobic nano-coatings, rear ventilation enhancement, passive cooling fins, Right Grid orientation recalibration, IoT fault monitoring, and soiling rate tracking. To address these specific power drops, we recommend.
6. The PRCLM framework can adopt agricultural and institutional rooftop PV installations across humid tropical South Asia where calibrated pyranometer data are unavailable. Results should be viewed with our specific dataset, assumptions, and data limitations in mind.

ACKNOWLEDGEMENTS

The authors sincerely acknowledge the support of the Management, Faculty, and Technical Staff of the Kelappaji College of Agricultural Engineering and Food Technology (KCAEFT), Kerala Agricultural University, Tavanur, Malappuram, for facilitating site access, instrumentation deployment, and data collection throughout the study period. The contribution of the Agency for Non-conventional Energy and Rural Technology (ANERT), Government of Kerala, in commissioning and maintaining the study installation is gratefully acknowledged.

All observational data were collected on-site and are reported without alteration. No external research funding was received for this study.

Conflict of Interest:

The authors declare no conflict of interest.

Funding and Acknowledgment:

No external research funding was received for this study. The authors sincerely acknowledge the support of the Management, Faculty, and Technical Staff of KCAEFT, Kerala Agricultural University, Tavanur, and the Agency for Non-conventional Energy and Rural Technology (ANERT), Government of Kerala, for facilitating site access, instrumentation deployment, and data collection.

Ethics Statement:

This study involved the monitoring of an existing solar photovoltaic installation using non-invasive instrumentation and publicly available inverter data. No human subjects, animals, or biological materials were involved. Ethical approval was not required for this research.

Originality and Plagiarism:

The authors confirm that this manuscript is an original work that has not been previously published and is not under consideration for publication elsewhere. A plagiarism check was conducted and the similarity index is 4%, which is within the acceptable limit.

Consent for Publication:

All authors have read and approved the final version of the manuscript and consent to its publication in the journal.

Competing Interests:

The authors declare no conflict of interest, financial or otherwise, that could have influenced the conduct or reporting of this research.

Data Availability:

The primary observational dataset (November 2024, n = 28 days) and the inverter-logged monthly generation data used in this study are available from the corresponding author (velmuruganv709@gmail.com) upon reasonable request.

Author Contributions:

Velmurugan E.: Conceptualization, field data collection, methodology development, formal analysis, writing — original draft, and visualization. Suma Nair: Supervision, methodology review, and writing — review and editing. Naveen S.: Field data collection, instrumentation support, and data curation.

REFERENCES

Ajub Ajulian ZM, Sinuraya EW and Winardi B 2025. The effect of temperature and weather conditions on the performance of photovoltaic modules in tropical Indonesia. *W. Sci. Inf. Syst. Technol.,* **3**: 84-91. https://doi.org/10.58812/wsist.v3i01.1246

Baghel NS and Chander N 2022. Performance comparison of mono and polycrystalline silicon solar photovoltaic modules under tropical wet and dry climatic conditions in east-central India. *Clean Energy,* **6**: 165-177. https://doi.org/10.1093/ce/zkac001

Bamisile O, Acen C, Cai D, Huang Q and Staffell I 2025. The environmental factors affecting solar photovoltaic output. *Renew. Sust. Energy Rev.,* **208**: 115073. https://doi.org/10.1016/j.rser.2024.115073

Ghosh A 2020. Soiling losses: A barrier for India's energy security dependency from photovoltaic power. *Challenges,* **11**: 9. https://doi.org/10.3390/challe11010009

Hua Y, Wei M, Yuan J, He W, Chen L and Gao Y 2024. The impact of climate change on solar radiation and photovoltaic energy yields in China. *Atmosphere,* **15**: 939. https://doi.org/10.3390/atmos15080939

Marion B, Adelstein J, Boyle K, Hayden H, Hammond B, Fletcher T, Canada B, Narang D, Kimber A, Mitchell L, Rich G and Townsend T 2008. Performance parameters for grid-connected PV systems. *Proc. 31st IEEE Photovolt. Spec. Conf.*.pp. 1601-1606. https://doi.org/10.1109/PVSC.2005.1488539

Qasim MA and Atyia TH 2023. Evaluating the impact of weather conditions on the effectiveness and performance of PV solar systems and inverters. *NTU J. Renew. Energy,* **5**: 34-46. https://doi.org/10.56286/ntujre.v5i1.551

Skoplaki E and Palyvos JA 2009. On the temperature dependence of photovoltaic module electrical performance: A review of efficiency/power correlations. *Sol. Energy,* **83**: 614-624. https://doi.org/10.1016/j.solener.2008.10.008

Wu X, Wang Y, Deng S and Su P 2025. Climate-responsive design of photovoltaic façades in hot climates: materials, technologies, and implementation strategies. *Buildings,* **15**: 1648. https://doi.org/10.3390/buildings15101648